Photoinduced Se−C Insertion Following Photolysis of (η^5-C_4H_4Se)$Cr(CO)_3$. A Picosecond and Nanosecond Time-Resolved Infrared, Matrix Isolation, and DFT Investigation

Peter Brennan,[†] Michael W. George,[‡] Omar S. Jina,[‡] Conor Long,[†] Jennifer McKenna,[†] Mary T. Pryce,*[,†] Xue-Zhong Sun,[‡] and Khuong Q. Vuong[‡]

School of Chemical Sciences, Dublin City University, Dublin 9, Ireland, and the School of Chemistry, University of Nottingham, University Park, Nottingham NG7 2RD, U.K.

Received November 28, 2007

The photochemistry of (η^5-C_4H_4Se)$Cr(CO)_3$ was investigated by matrix isolation, time-resolved infrared spectroscopy, and steady-state photochemical methods. Density functional theory (DFT) was used to assist in the identification of the photoproducts. Irradiation (λ_{exc}= 406 nm) of (η^5-C_4H_4Se)$Cr(CO)_3$ in either an Ar or CH_4 matrix at 20 K produced the selenophene ring-opened insertion product (*C,Se*-C_4H_4Se)$Cr(CO)_3$. Further irradiation of this matrix produced the CO-loss species (*C,Se*-C_4H_4Se)$Cr(CO)_2$. Pulsed irradiation at 400 nm produced the CO-loss species (η^5-C_4H_4Se)$Cr(CO)_2$(S) in *n*-heptane (S) along with the insertion products (*C,Se*-C_4H_4Se)$Cr(CO)_3$ and (*C,Se*-C_4H_4Se)$Cr(CO)_2$, both of which may have triplet character. Time-resolved measurements on the microsecond time scale confirmed that the CO-loss species (η^5-C_4H_4Se)$Cr(CO)_2$(S) reacts with CO ($k_2 = 5.8 \times 10^6$ dm^3 mol^{-1} s^{-1} at 298 K), while (*C,Se*-C_4H_4Se)$Cr(CO)_3$ and (*C,Se*-C_4H_4Se)$Cr(CO)_2$ do not react on this time scale. DFT calculations provide an explanation of the stability of the triplet (*C,Se*-C_4H_4Se)$Cr(CO)_3$ species in terms of a chromaselanabenzene structure, which is consistent with previously observed metal insertion into coordinated selenophene ligands.

Introduction

Hydrodesulfurization (HDS) is an important industrial process both in terms of reducing the environmental impact of the burning of fossil fuels and also in protecting the efficacy of industrial processes that depend on oil-based feed-stocks.[1] In the HDS process, sulfur, contained in a variety of organic compounds, is removed by treatment with H_2. The process depends on heterogeneous catalysts mainly based on group 6 metals supported on alumina. Various groups have probed the mechanism of the HDS process by studying the chemistry of metal complexes of thiophenes, benzothiophenes, and other sulfur-containing aromatic compounds.[2] Aromatic sulfur compounds are among the most difficult to treat with existing hydroprocessing technologies and require the more rigorous conditions of "deep" hydrodesulfurization. It is clear from these studies that the HDS process involves the initial coordination of the thiophene molecule to the metal atom followed by its insertion into the S−C bond. A range of coordination modes for the thiophene−metal interaction have been observed to date with hapticities ranging from η^1-*S* to η^1-*C*, η^2-, η^4-, and η^5-, as well as the insertion product.[3]

In earlier work we investigated the photochemistry of the heteroaromatic (η^6-C_5H_5N)$Cr(CO)_3$ and (η^5-C_5H_5)(η^5-C_4H_4N)Fe systems.[4,5] This work provided evidence that the π-bound pyridine or pyrrolyl ligands undergo haptotropic shifts following low-energy photolysis in both frozen gas matrixes and room-temperature solution. In addition, wavelength-dependent photochemistry was observed, with long-wavelength photolysis tending to favor haptotropic shifts, while higher energy irradiation produced CO-loss products in the case of the metal carbonyl system. This clearly indicates the presence of two classes of excited states, one leading to a change in the coordination mode of the heteroaromatic ligand and the other leading to the CO-loss process. Photoinduced changes to the coordination mode of π-bound ligands offer the exciting possibility of opening coordination sites on the metal that could mimic the vacant sites available on metal atoms in heterogeneous catalytic systems.

* Corresponding author. Fax: + 353 1 7005503. Tel: + 353 1 7008005. E-mail: mary.pryce@dcu.ie.

[†] Dublin City University.

[‡] University of Nottingham.

(1) For example: (a) Goodrich, J. D.; Nickias, P. N.; Selegue, J. P. *Inorg. Chem.* **1987**, *26*, 3426. (b) Bucknor, S. M.; Draganjac, M; Rauchfuss, T. B.; Ruffing, C. J. *J. Am. Chem. Soc.* **1984**, *106*, 5379. (c) Sanchez-Delgado, R. A.; Herrera, V.; Bianchini, C.; Masi, D.; Mealli, C. *Inorg. Chem.* **1993**, *32*, 3766. (d) Vecchi, P. A.; Ellern, A.; Angelici, R. J. *Organometallics* **2005**, *24*, 2168. (e) McKinley, S. G.; Vecchi, P. A.; Ellern, A.; Angelici, R. J. *Dalton Trans.* **2004**, *5*, 788. (f) Vecchi, P. A.; Ellern, A.; Angelici, R. J. *J. Am. Chem. Soc.* **2003**, *125*, 2064. (g) Startsev, A. N. *Catal. Rev.* **1995**, *37*, 353.

(2) (a) Bianchini, C.; Casares, J. A.; Osman, R.; Pattison, D. A.; Perutzzini, M.; Perutz, R. N.; Zanobini, F. *Organometallics* **1997**, *16*, 4611. (b) Bianchini, C.; Masi, D.; Meli, A.; Pertuzzini, M.; Vissa, F.; Zanobini, F. *Organometallics* **1998**, *17*, 2495. (c) Zhang, X.; Dullaghan, C. A.; Carpenter, G. B.; Sweigart, D. A.; Meng, Q. *J. Chem. Soc., Chem. Commun.* **1998**, 93. (d) Arévalo, A.; Bernès, S.; García, J. J.; Maitlis, P. M. *Organometallics* **1999**, *18*, 1680. (e) Chantson, J.; Görls, H.; Lotz, S. *J. Organomet. Chem.* **2003**, *687*, 39. (f) Reynolds, M. A.; Guzei, I. A.; Angelici, R. J. *J. Am. Chem. Soc.* **2002**, *124*, 1689. (g) Reynolds, M. A.; Guzei, I. A.; Angelici, R. J. *Organometallics* **2001**, *20*, 1071. (h) Li, H.; Yu, K.; Watson, E. J.; Virkaitis, K. L.; D'Acchioli, J. S.; Carpenter, G. B.; Sweigart, D. A.; Czech, P. T.; Overly, K. R.; Coughlin, F. *Organometallics* **2002**, *21*, 1262.

(3) (a) Angelici, R. J. *Bull. Soc. Chim. Belg.* **1995**, *104*, 265. (b) Chen, J.; Young, V. G., Jr.; Angelici, R. J. *J. Am. Chem. Soc.* **1995**, *117*, 6362.

(4) Breheny, C. J.; Draper, S. M.; Grevels, F.-W.; Klotzbücher, W. E.; Long, C.; Pryce, M. T.; Russell, G. *Organometallics* **1996**, *15*, 3679.

(5) Heenan, D. P.; Long, C.; Montiel-Palma, V.; Perutz, R. N.; Pryce, M. T. *Organometallics* **2001**, *19*, 3869.

10.1021/om7011979 CCC: $40.75
Publication on Web 07/16/2008

Table 1. Diagnostic IR Bands for (η^5-C_4H_4Se)$Cr(CO)_3$ and Photoproducts in Various Media

complex	ν_{CO} (cm^{-1})	$\nu_{N\equiv N}$ (cm^{-1})	medium
(η^5-C_4H_4Se)$Cr(CO)_3$	1989, 1924, 1901		*a*
	1977, 1906, 1884		*b*
	1982, 1916, 1891		*c*
	1982, 1914, 1893		*d*
	1983, 1914, 1896		*e*
	1983, 1918, 1897		*f*
(η^5-C_4H_4Se)$Cr(CO)_2$	1925, 1860		*f*
(η^5-C_4H_4Se)$Cr(CO)_2N_2$	1934, 1879	2172	*d*
^{3}(*C,Se*-C_4H_4Se)$Cr(CO)_3$	2046, 2001, 1957		*a*
	2044, 1996, 1953		*b*
	2044, 1997, 1953		*c*
	2039, 2000, 1959		*f*
(*C,Se*-C_4H_4Se)$Cr(CO)_2$	2014, 1954		*f*
	2014, 1956		*e*
^{3}(η^1-*C2*-C_4H_4Se)$Cr(CO)_3$	1981, 1911, 1891		*a*
$Cr(CO)_6$	1985		*b*[e]

[a] Argon at 20 K. [b] 5% CO in argon at 20 K. [c] Methane at 20 K. [d] Dinitrogen at 20 K. [e] Cyclohexane at room temperature. [f] *n*-Heptane at room temperature.

For this reason we have now extended these studies to include the photochemistry of (η^5-C_4H_4E)$Cr(CO)_3$ (E = S or Se). Selenophene has exhibited a similar range of coordination modes to thiophene.[6–8] In this paper we describe electronic structure and photochemical behavior of (η^5-C_4H_4Se)$Cr(CO)_3$. We have used theoretical methods, steady-state and pico- and nanosecond time-resolved infrared techniques, and low-temperature matrix isolation techniques to identify the various intermediates observed including the Se−C insertion product (*C,Se*-C_4H_4Se)$Cr(CO)_3$, which we propose has a ground-state triplet configuration. Harris et al.[9] have shown that complexes of the group 7 elements can activate Si−H bonds under photochemical conditions. This work demonstrated that the early time reaction dynamics depend on the electronic structure of the complexes. For instance excitation of (η^5-C_5H_5)$Mn(CO)_3$ produces (η^5-C_5H_5)$Mn(CO)_2$ in both the singlet and triplet state, and it is the triplet species that reacts more rapidly with the Si−H bond in trialkylsilanes.

Results

The IR spectroscopic data for (η^5-C_4H_4Se)$Cr(CO)_3$ and the observed photoproducts are given in Table 1. The UV−vis spectrum of (η^5-C_4H_4Se)$Cr(CO)_3$ in cyclohexane with features centered at 378, 416, and 520 nm is presented in Figure 1. In the case of time-resolved and matrix isolation spectra, data are presented in the form of difference absorbance in which the positive (upward) bands represent the appearance of new species while negative bands (downward bleaches) represent photoinduced depletion.

Quantum Chemical Calculations. DFT methods were used to calculate the electronic and molecular structures and the spectroscopic properties of compounds relevant to this study including the selenophene ligand, (η^5-C_4H_4Se)$Cr(CO)_3$, (η^5-C_4H_4Se)$Cr(CO)_2$, (η^1-*C2*-C_4H_4Se)$Cr(CO)_3$, and the insertion products (*C,Se*-C_4H_4Se)$Cr(CO)_3$ and (*C,Se*-C_4H_4Se)$Cr(CO)_2$ on both the singlet and triplet surfaces. In all cases starting structures were obtained from molecular mechanics, and these were then optimized without geometric constraints using tight convergence criteria (see Experimental Section).

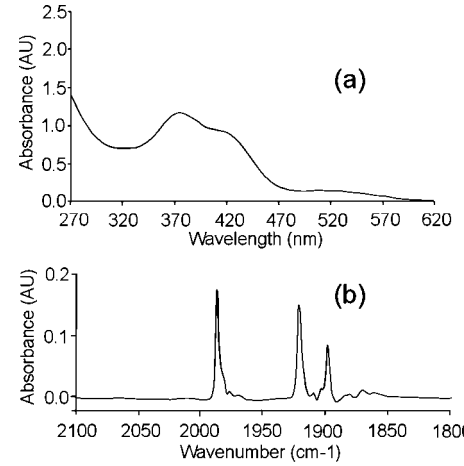

Figure 1. (a) UV/vis spectrum of (η^5-C_4H_4Se)$Cr(CO)_3$ in cyclohexane (2.5×10^{-4} mol dm^3) and (b) its IR spectrum in the ν_{CO} region showing peaks at 1989, 1924, and 1901 cm^{-1} obtained in an Ar matrix at 20 K.

The calculated molecular structure of (η^5-C_4H_4Se)$Cr(CO)_3$ was compared to that of the published molecular structure of (η^5-2,5-$(CH_3)_2C_4H_2Se$)$Cr(CO)_3$ obtained by single-crystal X-ray diffraction methods.[10] In general the calculated bond lengths for (η^5-C_4H_4Se)$Cr(CO)_3$ were similar to those of the dimethyl derivative with the exception of the Cr−Se bond length, where a calculated value of 2.63229 Å is significantly longer than the measured value of 2.488(5) Å. Table 2 contains selected bond lengths based on the calculated optimized structures. The calculated ν_{CO} band positions were calibrated using the measured positions of the parent compound (η^5-C_4H_4Se)$Cr(CO)_3$,[11] and this calibration was verified by comparison of the measured band positions of (η^5-C_4H_4Se)$Cr(CO)_2$(S) (S = *n*-heptane) with those calculated for (η^5-C_4H_4Se)$Cr(CO)_2$ (Table 5). DFT frequency calculations are sufficiently accurate to be used as a predictive tool, and an error of 1% is appropriate for the calculated band positions.[12]

The electronic structure of (η^5-C_4H_4Se)$Cr(CO)_3$ was calculated to provide a description of the bonding between the chromium tricarbonyl fragment and the selenophene ligand. For the (η^5-C_4H_4Se)$Cr(CO)_3$ complex the selenium atom lies out of the plane generated by the remaining four carbon atoms. The dihedral angle C4−C3−C2−Se is 10°, while the equivalent angle for the (η^1-C_4H_4Se)$Cr(CO)_3$ complex is 0.4° and the selenophene ligand is essentially planar. Furthermore the selenophene ligand is nonplanar in the measured structure of (η^5-2,5-$(CH_3)_2C_4H_2Se$)$Cr(CO)_3$; the dihedral angle between the plane defined by the four ring carbons and the plane defined by the Se, C2, and C5 atoms is 6.7(6)°.

A model for the electronic structure of (η^5-C_4H_4Se)$Cr(CO)_3$ was obtained from DFT calculations at the B3LYP/LANL2DZ+p level. The percent contributions of the Cr, Se, ring CH units, and CO ligands to the Kohn−Sham orbitals are presented in Table 3. Surprisingly, there is little evidence for a substantial overlap of Cr and Se atomic orbitals in the valence Kohn−Sham

(6) (a) Choi, M. G.; Angelici, R. J. *J. Am. Chem. Soc.* **1990**, *112*, 7811. (b) Choi, M. G.; Angelici, R. J. *J. Am. Chem. Soc.* **1991**, *113*, 5651. (c) White, C. J.; Angelici, R. J.; Choi, M. G. *Organometallics* **1995**, *14*, 332.
(7) Angelici, R. J. *Coord. Chem. Rev.* **1990**, *105*, 61.
(8) Angelici, R. J. *Organometallics* **2001**, *20*, 1259.
(9) Yang, H.; Kotz, K. T.; Asplund, M. C.; Harris, C. B. *J. Am. Chem. Soc.* **1997**, *119*, 9564.
(10) White, C. J.; Angelici, R. J.; Choi, M-G. *Organometallics* **1995**, *14*, 332.
(11) Calculated band maxima for (η^5-C_4H_4Se)$Cr(CO)_3$: 1944, 1887, and 1874 cm^{-1}; observed: 1983, 1918, 1897 cm^{-1}; linear regression analysis yielded a best fit line $y = 1.202x - 353.08$, $r^2 = 0.9963$.
(12) Zaric, S.; Hall, M. B. *J. Phys. Chem.* **1998**, *102*, 1963.

Table 2. Selected Bond Lengths (Å) in (η^5-2,5-$(CH_3)_2C_4H_2Se$)$Cr(CO)_3$ (X-ray diffraction data from ref 10) and Calculated Values (B3LYP/LANL2DZ+p) for (η^5-C_4H_4Se)$Cr(CO)_3$ (singlet and triplet), (η^1-*C2*-C_4H_4Se)$Cr(CO)_3$ (singlet), and (*C,Se*-C_4H_4Se)$Cr(CO)_3$ (singlet and triplet)

	multiplicity	Cr−Se (Å)	Cr−CO(Å)			Cr−C2(selenophene) (Å)
(η^5-2,5-$(CH_3)_2C_4H_2Se$)$Cr(CO)_3$		2.488(5)	1.829(6)	1.822(6)	1.835(6)	2.218(6)
(η^5-C_4H_4Se)$Cr(CO)_3$	singlet	2.632298	1.840536	1.823097	1.840531	2.233076
^{3}(η^5-C_4H_4Se)$Cr(CO)_3$	triplet	2.994299	1.864645	1.911865	1.864631	2.326914
(η^1-*C2*-C_4H_4Se)$Cr(CO)_3$	singlet	2.894510	1.913191	1.842648	1.911825	2.136325
(*C,Se*-C_4H_4Se)$Cr(CO)_3$	singlet	2.408461	1.909538	1.830132	1.870209	1.939063
^{3}(*C,Se*-C_4H_4Se)$Cr(CO)_3$	triplet	2.450389	2.030335	1.896888	1.920339	1.956775

Table 3. Percent Contributions of the Cr, CO, Se, and CH Units to the Highest Occupied Kohn−Sham Orbital (HOKS) along with the 10 Highest Energy Orbitals Calculated at the B3LYP/LANL2DZ+p Level of Theory

			% contribution			
number	name	energy (eV)	Cr	CO's	Se	CH's
45	HOKS	−6.04	65	27	1	6
44	H-1	−6.18	60	25	6	10
43	H-2	−6.29	68	25	3	4
42	H-3	−8.6	9	3	58	30
41	H-4	−8.76	13	4	1	82
40	H-5	−10.64	4	44	24	28
39	H-6	−10.8	6	44	9	41
38	H-7	−10.9	14	83	0	3
37	H-8	−11.02	12	37	31	20
36	H-9	−11.21	0	13	27	60
35	H-10	−11.38	1	89	3	7

orbitals with the exception of orbital 37. A pictorial representation of this orbital is presented in Figure 2. Recently the valence shell electronic structure of selenophene (C_{2v}) has been presented at the Hartree−Fock level.[13] A frontier orbital approach to describing the bonding in (η^5-C_4H_4Se)$Cr(CO)_3$ suggests that the selenophene orbital contributing to orbital 37 has the same symmetry as that of the $6a_1$ orbital of the selenophene ligand (Figure 2C). This orbital describes part of the bonding interaction between the selenium atom and the C2 and C5 atoms. Consequently, the coordination of the selenophene ligand to the electron-deficient chromium tricarbonyl fragment has the effect of reducing the bond order between the selenium and the adjacent carbons in the selenophene ring. This explains why the Se−C bond lengths are slightly longer in (η^5-2,5-$(X)_2$-C_4H_2Se)$Cr(CO)_3$ (1.899(8) and 1.912(7) Å measured for X = CH_3:[10] 1.95670 Å calculated for X = H) than in the uncoordinated selenophene ligand (1.855(7) Å).[14] Consequently the interaction of the selenophene ligand with the chromium tricarbonyl fragment can be described as a four-electron interaction with the four ring carbons plus a weak two-electron interaction with the C2−Se−C5 fragment. Comparisons of the Mulliken charges on the chromium and selenium atoms are presented in Table 4. The Mulliken charge on the chromium atom is significantly less in (η^5-C_4H_4Se)$Cr(CO)_3$ than in (η^6-C_6H_6)$Cr(CO)_3$. In addition the charge on the selenium atom increases significantly upon coordination to the chromium tricarbonyl fragment.

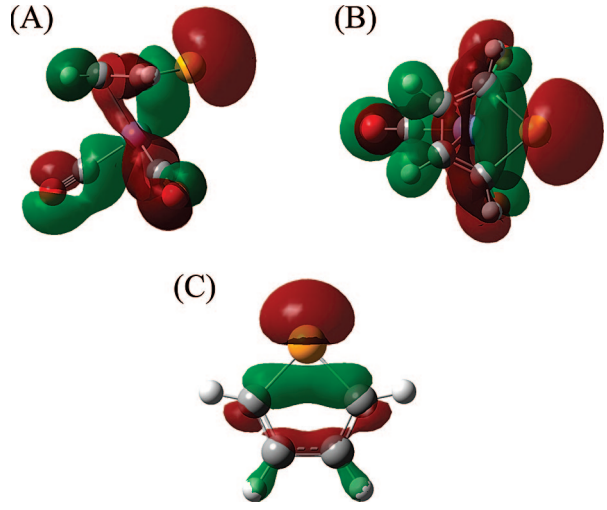

Figure 2. Pictorial representation of Kohn−Sham orbital number 37 showing the distortion of the selenophene ring from planarity to accommodate the interaction between the orbitals on the chromium and selenium atoms: (A) side view; (B) top view. (C) Representation of the $6a_1$ occupied orbital on the selenophene ligand.

A number of possible reduced hapticity species were probed in this study; however the only species to be located at a local minimum was (η^1-*C2*-C_4H_4Se)$Cr(CO)_3$. Table 2 contains some structural parameters for the various species identified in these studies, with full structural parameters available in the Supporting Information. Figure 3 shows how the triplet energies of the (η^5-C_4H_4Se)$Cr(CO)_3$ and (η^1-*C2*-C_4H_4Se)$Cr(CO)_3$ complexes are higher than those of the equivalent singlet species, and this contrasts with the insertion product, where the triplet energy is estimated to be some 2 kJ mol^{-1} lower than that of the singlet at this model chemistry. It should be noted that DFT methods can often underestimate triplet energies compared to the MP2 level of theory[15] and that the exchange functional used in the B3LYP method can result in considerable errors in singlet−triplet energy level splittings.[16]

Time-dependent density functional theory was used to determine the prevailing character of the optically accessible excited states of the (η^5-C_4H_4Se)$Cr(CO)_3$ species. The 20 lowest energy vertical perturbations were investigated, and the character of each transition was defined in the following terms: metal-to-ligand charge transfer (either selenophene or carbonyl ligands) (MLCT) or metal-based ligand field (LF) transitions. The results of these calculations are presented in Table 6. It can be seen that the prevailing character of the low-energy absorption band consists of transitions that are predominantly MLCT in character with a substantial portion of the charge transfer to the selenophene ligand. Higher energy absorptions, predicted at 368 nm, contain significant LF with some MLCT character, the charge transferring to the carbonyl ligands. Consequently, the preferred experimental approach to the photochemical studies was to conduct initial photolyses at wavelengths greater than 368 nm, followed, where possible, by higher energy irradiation.

(13) Powis, I.; Zaytseva, I. L.; Trofimov, A. B.; Schirmer, J.; Halland, D. M. P.; Potts, A. W.; Karlsson, L. *J. Phys. B: At. Mol. Opt. Phys.* **2007**, *40*, 2019.

(14) (a) Bird, C. W.; Cheeseman, G. W. H.; Hornfeldt, A. B. In *Comprehensive Heterocyclic Chemistry*; Katritzky, A. R., Rees, C. W., Eds.; Pergamon Press: New York, Vol *4*; pp 935−971. (b) Brown, R. D.; Burden, F. R.; Godfrey, P. D. *J. Mol. Spectrosc.* **1968**, *25*, 415.

(15) Snee, P. T.; Yang, H.; Kotz, K. T.; Payne, C. K.; Harris, C. B. *J. Phys. Chem.* **1999**, *103*, 10426.

(16) (a) Sorkin, A. S.; Iron, M. A.; Truhlar, D. G. *J. Chem. Theory Comput.* **2008**, *4*, 307. (b) Reiher, M. *Inorg. Chem.* **2002**, *41*, 6928.

Table 4. Mulliken Charges on Selected Atoms in Some Reference Systems, the Selenophene Ligand, and (η^6-C_6H_6)Cr(CO)$_3$, along with Those Obtained for (η^5-C_4H_4Se)Cr(CO)$_3$, (η^1-*C2*-C_4H_4Se)Cr(CO)$_3$, and the Insertion Products (*C,Se*-C_4H_4Se)Cr(CO)$_3$ and (η^5-C_4H_4Se)Cr(CO)$_2$ on the Singlet and Triplet Surfaces

compound	multiplicity	Mulliken charge[a] on Cr	Se	C2	C3
C_4H_4Se	singlet		0.04685	−0.320648	−0.169482
(η^6-C_6H_6)Cr(CO)$_3$	singlet	−0.166891		−0.21962[b]	
(η^5-C_4H_4Se)Cr(CO)$_3$	singlet	−0.042252	0.463214	−0.584768	−0.135685
	triplet	0.028272	0.391798	−0.590358	−0.157867
(η^1-*C2*-C_4H_4Se)Cr(CO)$_3$	singlet	0.165727	0.409615	−0.731977	−0.091294
	triplet	0.26246	0.402716	−0.70922	−0.128253
(*C,Se*-C_4H_4Se)Cr(CO)$_3$	singlet	0.044853	0.205979	−0.296377	−0.141831
	triplet	0.283467	0.058224	−0.352846	−0.196357
(η^5-C_4H_4Se)Cr(CO)$_2$	singlet	0.220994	0.423157	−0.585726	−0.162812
	triplet	0.226275	0.431148	−0.602686	−0.151929

[a] Obtained from B3LYP/LANL2DZ+p calculations. [b] Average charge on benzene carbons.

Table 5. Calculated ν_{CO} Peak Positions with the Observed Peaks in Parentheses for (η^5-C_4H_4Se)Cr(CO)$_3$ and Its Photoproducts

compound	multiplicity	ν_{CO} (cm^{-1})		
(η^5-C_4H_4Se)Cr(CO)$_3$	singlet	1984	1915	1899
		(1983)[a]	(1918)[a]	(1897)[a]
	triplet	1987	1925	1884
(η^1-*C2*-C_4H_4Se)Cr(CO)$_3$	singlet	1976	1890	1880
	triplet	1981	1914	1877
		(1981)	(1911)	(1891)
(*C,Se*-C_4H_4Se)Cr(CO)$_3$	singlet	2025	1974	1942
	triplet	2050	1988	1963
		(2046)[b]	(2001)[b]	(1957)[b]
		(2039)[a]	(2000)[a]	(1959)[a]
(η^5-C_4H_4Se)Cr(CO)$_2$	singlet	1939	1882	
		(1925)[a]	(1860)[a]	
(*C,Se*-C_4H_4Se)Cr(CO)$_2$	singlet	2008	1920	
	triplet	2023	1948	
		(2014)[a]	(1954)[a]	
		(2014)[c]	(1956)[c]	
		(2035)[b]	(1934)[b]	

[a] *n*-Heptane solution at room temperature. [b] Argon matrix at 20 K. [c] Cyclohexane at room temperature.

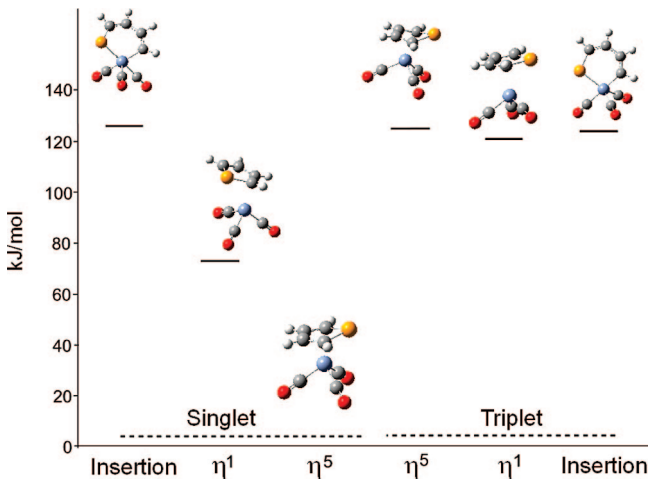

Figure 3. Energies of (η^1-*C2*-C_4H_4Se)Cr(CO)$_3$ and (*C,Se*-C_4H_4Se)Cr(CO)$_3$ on the singlet and triplet surfaces relative to the energy of the singlet (η^5-C_4H_4Se)Cr(CO)$_3$ set at zero at the B3LYP/LANL2DZ+P level. The authors are grateful to one referee, who urged caution in the analysis of the energy differences between the singlet and triplet species at this level of theory.[16]

Photolysis of (η^5-C_4H_4Se)Cr(CO)$_3$ in an Ar or CH_4 Matrix at 20 K. The IR spectrum for (η^5-C_4H_4Se)Cr(CO)$_3$ in all matrixes confirms that the Cr(CO)$_3$ fragment has local C_s symmetry, resulting in three ν_{CO} bands. Because the behavior following photolysis of (η^5-C_4H_4Se)Cr(CO)$_3$ in both Ar or CH_4 matrixes was essentially identical, description of the results of these experiments is limited to those obtained in Ar. Initial photolysis (λ_{exc} = 405 nm or >410 nm) of (η^5-C_4H_4Se)Cr(CO)$_3$ in an Ar matrix reduced the intensity of the parent bands at 1989, 1924, and 1901 cm^{-1} with concomitant formation of bands at 2046, 2001, and 1957 cm^{-1}. An IR difference spectrum of these changes is presented in Figure 4a. The relative intensities of the three product bands remained constant, and therefore they were assigned to a single species containing three CO ligands. On the basis of the similarity of these peak positions to those calculated for the triplet Se−C insertion product (Table 5) and its reactivity (described later) these peaks were assigned to ^{3}(*C,Se*-C_4H_4Se)Cr(CO)$_3$. Subsequent long-wavelength irradiation with λ_{exc} > 500 nm decreased the intensity of the

Table 6. Calculated Vertical Excitation Energies for the Five Lowest Energy Transitions (eV) with the Equivalent Excitation Wavelength (nm) Oscillator Strength (*f*) and Prevailing Character for the Transitions (singlet excited states only)

eV	nm	*f*	prevailing character
2.3423	529.32	0.0041	MLCT[a]
2.5570	484.87	0.0012	MLCT[a]
2.9330	422.73	0.0356	MLCT[a]
3.3699	367.91	0.0207	MLCT[b], LF
3.3704	367.86	0.0004	MLCT[a]

[a] Transitions with a major contribution from metal to selenophene charge transfer. [b] Transitions with a major contribution from metal to carbonyl charge transfer.

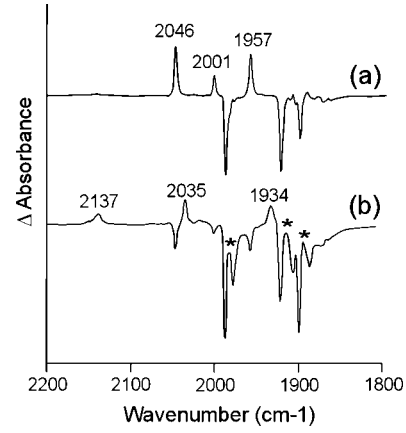

Figure 4. (a) IR difference spectrum indicating the changes observed following photolysis (λ_{exc} = 406 nm) of (η^5-C_4H_4Se)Cr(CO)$_3$ in an argon matrix at 20 K. (b) IR difference spectrum obtained following subsequent photolysis of matrix in (a) with 320 < λ_{exc} < 390 nm at 20 K; peaks marked with * are assigned to ^{3}(η^1-*C2*-C_4H_4Se)Cr(CO)$_3$ (1981, 1911, and 1891 cm^{-1}) on the basis of the similarity of these band positions to those predicted for this species by DFT methods.

product bands with re-formation of the bands of the parent (η^5-C_4H_4Se)$Cr(CO)_3$ (reaction 1). Thus under these conditions the matrix exhibits a photochromic behavior.

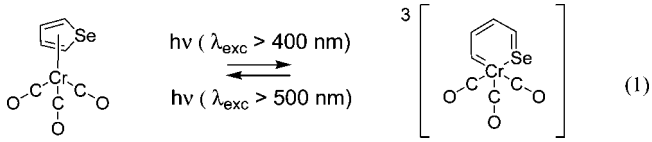

(1)

Photolysis of this matrix with $\lambda_{exc} = 365$ nm led to a decrease in intensity of the parent bands and also those of (*C,Se*-C_4H_4Se)$Cr(CO)_3$, but new bands at 2137, 2035, and 1934 cm^{-1} (Figure 4b) appeared. The band at 2137 cm^{-1} was assigned to uncoordinated or "free" CO in the matrix, and the bands at 2035 and 1934 cm^{-1} were assigned to the 14-electron ^{3}(*C,Se*-C_4H_4Se)$Cr(CO)_2$ species on the basis of the similarity of the observed band positions to the calculated values (Table 5, reaction 2). In addition peaks at 1981, 1911, and 1891 cm^{-1} (marked with * in Figure 4b) were produced that are consistent with the calculated peak positions of ^{3}(η^1-C_4H_4Se)$Cr(CO)_3$ (Table 5). Surprisingly no evidence for the formation of (η^5-C_4H_4Se)$Cr(CO)_2$ was obtained in these experiments.

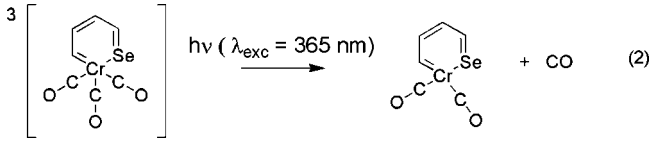

(2)

Photolysis of (η^5-C_4H_4Se)$Cr(CO)_3$ in a Dinitrogen Matrix at 20 K. As previously described for both Ar and CH_4 matrixes, initial irradiation at either $\lambda_{exc} = 405$ nm or >410 nm in a N_2 matrix produced ^{3}(*C,Se*-C_4H_4Se)$Cr(CO)_3$. The band positions were identical to those observed in either argon or methane, which indicates that the 16-electron ^{3}(*C,Se*-C_4H_4Se)$Cr(CO)_3$ species does not interact with the matrix medium.

When this matrix was subsequently photolyzed with $\lambda_{exc} =$ 365 nm, four new absorption bands appeared in the matrix at 2172, 2137, 1934, and 1879 cm^{-1}. The band at 2137 cm^{-1} was assigned to "free" CO in the matrix. The remaining bands at 2172 (ν_{NN}), 1934, and 1879 cm^{-1} are assigned to the dicarbonyl compound (η^5-C_4H_4Se)$Cr(CO)_2(N_2)$. The ν_{CO} bands are at lower energy than the bands of the parent bands and are consistent with a simple CO loss from (η^5-C_4H_4Se)$Cr(CO)_3$, analogous to the photoinduced CO loss from other (η-arene)$Cr(CO)_3$ systems (reaction 3).[17]

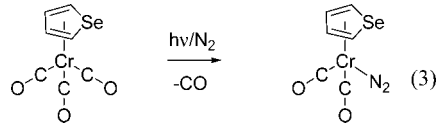

(3)

Pulsed Photolysis of (η^5-C_4H_4Se)$Cr(CO)_3$ in CO-Saturated Cyclohexane at Room Temperature. A solution of (η^5-C_4H_4Se)$Cr(CO)_3$ in CO-saturated cyclohexane was irradiated at $\lambda_{exc} = 355$ nm (pulsed Nd:YAG laser 35 mJ $pulse^{-1}$, repetition rate 1 Hz, exposure time 4.5 min), and the changes in the IR spectrum were monitored. The bands of the parent compound were reduced in intensity, and new bands were observed at 2014, 1985, and 1956 cm^{-1} (Figure 5). The band

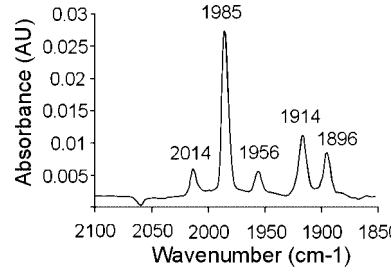

Figure 5. Room-temperature pulsed photolysis ($\lambda_{exc} = 355$ nm) of (η^5-C_4H_4Se)$Cr(CO)_3$ (1983, 1914, and 1896 cm^{-1}) in CO-saturated cyclohexane showing the formation of $Cr(CO)_6$ (1985 cm^{-1}) and a species containing the (*C,Se*-C_4H_4Se)Cr moiety (2014 and 1956 cm^{-1}).

at 1985 cm^{-1} was assigned to $Cr(CO)_6$, while those at 2014 and 1956 cm^{-1} are similar to those calculated for ^{3}(*C,Se*-C_4H_4Se)$Cr(CO)_2$ and a species with similar band positions was also observed in the time-resolved measurements (see below). The precise identity of this species cannot be confirmed from these measurements alone, but it is clear that photolysis results in loss of selenophene and generation of $Cr(CO)_6$.

Steady-State Photolysis of (η^5-C_4H_4Se)$Cr(CO)_3$ in CO-Saturated Perdeuterio Cyclohexane at Room Temperature. A solution of (η^5-C_4H_4Se)$Cr(CO)_3$ in C_6D_{12} was degassed by three cycles of freeze−pump−thaw in a NMR tube, after which 1 atm of CO was admitted. The resulting solution was examined by ^{1}H NMR spectroscopy (400 MHz). Two peaks were observed for this compound at chemical shifts of 5.4 and 5.5 ppm with respect to the TMS standard. The sample was then exposed to broadband (λ_{exc} > 340 nm; 200 W Xe lamp) irradiation external to the NMR cavity for a total of 50 min. During this time the tube was periodically transferred to the magnet cavity, and the NMR spectrum was obtained (Figure 6). These spectra showed a reduction in the intensity of the (η^5-C_4H_4Se)$Cr(CO)_3$ signals and the production of peaks at 7.36 and 7.54 ppm, which correspond to uncoordinated C_4H_4Se. In addition four peaks at 5.80, 6.25, 7.08, and 7.84 were assigned to an insertion product containing the (*C,Se*-C_4H_4Se)Cr moiety. During the course of the photolysis the quality of the spectra steadily deteriorated, indicating the formation of a high-spin species. Upon completion of the photolysis, the solvent was removed under reduced pressure and the residual orange solid was dissolved in degassed *n*-pentane. The IR spectrum of the resulting solution was obtained. Peaks observed at 1983, 1916, and 1899 cm^{-1} were assigned to unreacted (η^5-C_4H_4Se)$Cr(CO)_3$, a peak at 1985 cm^{-1} indicated the presence of $Cr(CO)_6$, and peaks at 2014 and 1956 cm^{-1} are consistent with the IR results obtained above.

Steady-State Photolysis of (η^5-C_4H_4Se)$Cr(CO)_3$ in Cyclohexane Containing a 5 M Excess of Pyridine at Room Temperature. A solution containing (η^5-C_4H_4Se)$Cr(CO)_3$ (2.2×10^{-4} M) and pyridine ([py] = 1.1×10^{-3} M) in cyclohexane was photolyzed (λ_{exc}= 355 nm). The spectral changes in the UV/vis spectrum indicated the decay of the parent compound (η^5-C_4H_4Se)$Cr(CO)_3$ ($\lambda_{max} = 370$ nm) with the formation of a compound absorbing at 418 nm (see Supporting Information). The presence of an isosbestic point at 366 nm indicates that this photochemical process is uncomplicated by side or subsequent reactions of the products. The IR spectrum of the photolysis solution was also examined. Interestingly no evidence for the formation of the insertion products ^{3}(*C,Se*-C_4H_4Se)-$Cr(CO)_3$ or (*C,Se*-C_4H_4Se)$Cr(CO)_2$ were obtained in these

(17) Creaven, B. S.; George, M. W.; Ginzburg, A. G.; Hughes, C.; Kelly, J. M.; Long, C.; McGrath, I. M.; Pryce, M. T. *Organometallics* **1993**, *12*, 3127.

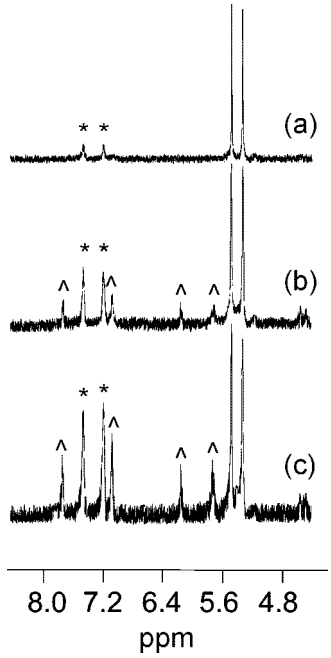

Figure 6. NMR spectra obtained (a) following freeze−pump−thaw degassing plus the addition of 1 atm of CO of a solution of (η^5-C_4H_4Se)$Cr(CO)_3$ in C_6D_{12}, (b) after 25 min photolysis with a 200 W Xe lamp fitted with a 340 nm cutoff filter, and (c) after 55 min photolysis under the same conditions as in (b). Peaks marked with * are C_4H_4Se, while those marked with ^ are assigned to a (C,Se−C_4H_4Se)Cr moiety. A steady decline in the quality of these spectra during the course of this experiment confirms the formation of triplet species during the photochemical process.

experiments. Instead three main features were observed in the ν_{CO} region centered at 1978, 1916, and 1857 cm^{-1}. Both of the features at 1978 and 1857 consist of two unresolved bands, while the more intense feature at 1916 cm^{-1} consists of many overlapping bands, one of which is observed as a shoulder on the high-energy side. By comparison with the behavior of (η^6-C_6H_6)$Cr(CO)_3$, where photolysis in the presence of py produced (η^6-C_6H_6)$Cr(CO)_2$(py) with ν_{CO} bands at 1902 and 1850 cm^{-1}, the features at 1916 and 1857 cm^{-1} were assigned to (η^5-C_4H_4Se)$Cr(CO)_2$(py).[18] The two sets of features for this species arise from the possible rotamers for this complex. The remaining features at 1978 and two under the intense feature at 1916 cm^{-1} have been tentatively assigned to (*C,Se*-C_4H_4Se)$Cr(CO)_2$(py). Py is known to quench the triplet states of organic carbonyl compounds,[19] and it is plausible to propose the quenching of either the initially produced triplet species, ^{3}(*C,Se*-C_4H_4Se)-$Cr(CO)_2$, by py followed by reaction with py or simple reaction of ^{1}(*C,Se*-C_4H_4Se)$Cr(CO)_2$ with py.

Picosecond Time-Resolved Infrared Investigation of (η^5-C_4H_4Se)$Cr(CO)_3$ in *n*-heptane at Room Temperature (λ_{exc} = 400 nm). Pulsed photolysis of (η^5-C_4H_4Se)$Cr(CO)_3$ (λ_{exc} = 400 nm) produced an immediate bleach of the bands of (η^5-C_4H_4Se)$Cr(CO)_3$. Broad, featureless absorptions were produced within 1 ps (Figure 7). Over 1000 ps the parent bands recovered to approximately 90% of the initial bleach, while sharper product features emerged through vibrational cooling (Figure 8). Two of these peaks (1925 and 1860 cm^{-1}) are assigned to the CO-loss species (η^5-C_4H_4Se)$Cr(CO)_2$ (Table 5). Additional features

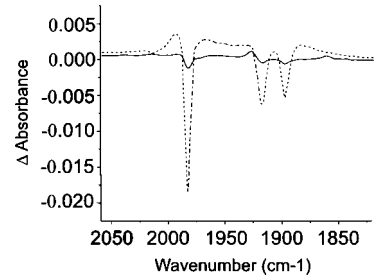

Figure 7. Picosecond infrared spectra obtained following picosecond photolysis of (η^5-C_4H_4Se)$Cr(CO)_3$ in CO-saturated *n*-heptane showing depletion and rapid recovery of the parent bands (approximately 90%) and the production of broad vibrationally hot bands. The spectrum indicated by dashed lines was obtained 3 ps after excitation (λ_{exc} = 400 nm); the solid line spectrum was obtained 1000 ps after excitation and is presented with an expanded scale in Figure 8.

were observed at 2039, 2014, 2000, 1959, and 1954 cm^{-1}. Of these, the peaks at 2039, 2000, and 1959 cm^{-1} correspond to the insertion product ^{3}(*C,Se*-C_4H_4Se)$Cr(CO)_3$ and are close to those observed in an argon matrix (see above). The peaks at 2014 and 1954 cm^{-1} can be assigned to (*C,Se*-C_4H_4Se)$Cr(CO)_2$, as these peaks are close to those observed following photolysis of ^{3}(*C,Se*-C_4H_4Se)$Cr(CO)_3$ in an argon matrix.

Nanosecond Time-Resolved Infrared Investigation of (η^5-C_4H_4Se)$Cr(CO)_3$ in CO-Saturated *n*-Heptane (S) at Room Temperature (λ_{exc} = 355 nm). Pulsed photolysis of (η^5-C_4H_4Se)$Cr(CO)_3$ (λ_{exc} = 355 nm) monitored on the nanosecond time scale resulted in an instantaneous depletion of the parent bands at 1983, 1917, and 1897 cm^{-1}. Seven product bands were observed at 2039, 1999, and 1959 cm^{-1} assigned to ^{3}(*C,Se*-C_4H_4Se)$Cr(CO)_3$, 2014 and 1954 cm^{-1} assigned to (*C,Se*-C_4H_4Se)$Cr(CO)_2$, and 1925 and 1860 cm^{-1} assigned to (η^5-C_4H_4Se)$Cr(CO)_2$(S) (S = heptane). Over the subsequent 15 μs the bands of the (η^5-C_4H_4Se)$Cr(CO)_2$ species decayed with a slight recovery of the depleted parent bands (Figure 9). Kinetic analysis of the decay of the 1860 cm^{-1} band yielded a rate constant (*k*) of 5.8 × 10^6 dm^3 mol^{-1} s^{-1} for the reaction of (η^5-C_4H_4Se)$Cr(CO)_2$(S) with CO (reaction 4) at 298 K. All other bands persist to over 15 μs, indicating that neither ^{3}(*C,Se*-C_4H_4Se)$Cr(CO)_3$ nor (*C,Se*-C_4H_4Se)$Cr(CO)_2$ react significantly with CO on this time scale, and both appear to be "spin blocked" to reaction with CO.

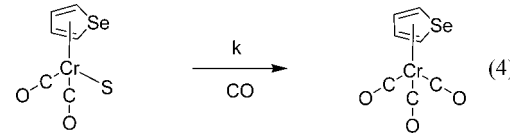

(4)

Discussion

The time-dependent DFT calculations suggest that excitation of (η^5-C_4H_4Se)$Cr(CO)_3$ at 400 nm will populate a metal to selenophene charge transfer excited state. Picosecond IR measurements show that the excited-state species is vibrationally hot, as indicated by the broad, featureless absorbances in Figure 7. It is only after 1000 ps that discrete features emerge. Two peaks (1925 and 1860 cm^{-1}) can be assigned to the CO-loss species (η^5-C_4H_4Se)$Cr(CO)_2$(S) because of the similarity of these peaks to those of known CO-loss species from other (η-arene)$Cr(CO)_3$ systems.[17] The fact that this species reacts with CO with a rate constant (5.8 × 10^6 dm^3 mol^{-1} s^{-1} at 298 K) that is similar to other 16-electron (η-arene)$Cr(CO)_2$ species in

(18) Pryce, M. T.The Photochemistry of (η^6-arene)$M(CO)_3$ (M = Cr or Mo) and Related Compounds. Ph.D. Thesis, Dublin City University, 1994.

(19) Zalesskaya, A.; Smabor, E. G.; Belý, N. N. *Opt. Spectrosc.* **2004**, *96*, 503.

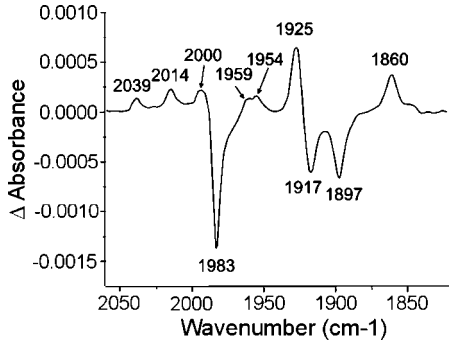

Figure 8. IR difference spectrum obtained 1 ns after excitation at 400 nm showing the vibrationally cool intermediates ^{3}(*C,Se*-C_4H_4Se)$Cr(CO)_3$ at 2039, 2000, and 1959 cm^{-1}, ^{3}(*C,Se*-C_4H_4Se)$Cr(CO)_2$ at 2014 and 1954 cm^{-1}, and (η^5-C_4H_4Se)$Cr(CO)_2$(*n*-heptane) at 1925 and 1860 cm^{-1}.

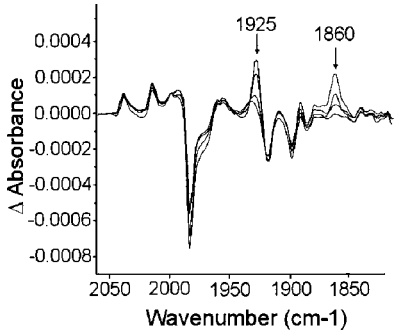

Figure 9. Difference IR spectra obtained following photolysis of (η^5-C_4H_4Se)$Cr(CO)_3$ in CO-saturated *n*-heptane showing the decay of the peaks of (η^5-C_4H_4Se)$Cr(CO)_2$(*n*-heptane) (1925 and 1860 cm^{-1}) as it reacts with CO to regenerate (η^5-C_4H_4Se)$Cr(CO)_3$; the remaining features remain unaffected and thus do not react with CO on this time scale (spectra obtained at 0.3,1.05, 4.9, and 15 μs after the excitation pulse).

alkane solvents supports this assignment.[17] It is the remaining features emerging after 1000 ps that distinguish the photochemical behavior of (η^5-C_4H_4Se)$Cr(CO)_3$ from other (η-arene)$Cr(CO)_3$ systems. Five peaks develop over 1000 ps, which can be assigned to two species, and these persist into the microsecond time domain. The first of these, absorbing at 2039, 2000, and 1959 cm^{-1}, is assigned to the C−Se insertion product (*C,Se*-C_4H_4Se)$Cr(CO)_3$, which exists in a triplet ground state, ^{3}(*C,Se*-C_4H_4Se)$Cr(CO)_3$. This assignment is based on the similarity of the peak positions with those calculated by DFT (Table 5) methods and the observation of similar peaks following 406 nm photolysis of (η^5-C_4H_4Se)$Cr(CO)_3$ in low-temperature matrixes (Figure 4a). The second species is also produced with ν_{CO} bands at 2014 and 1954 cm^{-1}. This species is assigned to (*C,Se*-C_4H_4Se)$Cr(CO)_2$ on the basis of the results of DFT calculations (Table 5) and the observation that ^{3}(*C,Se*-C_4H_4Se)$Cr(CO)_3$ undergoes photoinduced CO loss in an Ar matrix at 20 K, producing (*C,Se*-C_4H_4Se)$Cr(CO)_2$, which has similar IR characteristics. The TRIR and matrix isolation experiments confirmed that neither of these insertion products reacts with the medium nor with added CO. Although it is tempting to assign the species observed in the steady-state FTIR experiments outlined above, it is possible that these bands may be formed via subsequent reactions occurring on time scales between these measurements. Further studies are in progress in order to confirm the identity of this long-lived species. Thus, it is possible that these species may be "spin blocked" toward reaction with singlet species.[20a–c] Reiher has proposed that a reparameterized B3LYP functional (dubbed B3LYP*), in which the exact exchange coefficient is reduced from 0.2 to 0.15, yields better estimates of high-spin/low-spin energy splittings in organometallic systems.[20d,e] Calculations on (η^5-C_4H_4Se)$Cr(CO)_3$ using the B3LYP* functional, coupled with a triple-ζ basis set (TZVP), indicate that the triplet of this species lies some 120 kJ mol^{-1} above the singlet (zero-point energy corrections were applied). In contrast, the triplet of (*C,Se*-C_4H_4Se)$Cr(CO)_2$ was calculated to lie some 25 kJ mol^{-1} below the singlet at the same model chemistry, while the energies of the singlet and triplet (*C,Se*-C_4H_4Se)$Cr(CO)_3$ appear to be very close. However, it should be noted that bonding of the dicarbonyl to the alkane can be significant (40–50 kJ/mol^{-1}) and this complicates the assignment of (*C,Se*-C_4H_4Se)$Cr(CO)_2$ to either a singlet or a triplet.

The insertion of a transition metal into the Se−C bond in selenophene has been observed previously.[10] Treatment of [(η^5-2,5-$(CH_3)_2C_4H_2Se$)IrCp*]$^{2+}$ with 2 equiv of Na[$(CH_3OC_2H_4O)_2AlH_2$] produced (*C,Se*-2,5-$(CH_3)_2C_4H_2Se$)IrCp*, an iridaselenabenzene product in which the IrCp* unit is inserted into the Se−C bond of the selenophene (Cp* = $C_5(CH_3)_5$). NMR studies on this complex confirmed that it had significant aromatic character. The analogous thio compound is also known.[3b] However this is the first example of a photoinduced insertion of a $Cr(CO)_3$ fragment into a heteroaromatic ring.

The DFT calculations provide some explanation for the stability of the Se−C insertion product. Comparison of the Mulliken charges on the selenium atom in the uncoordinated selenophene with that of the coordinated ligand indicates that the selenium atom is more electron deficient when selenophene is coordinating to the chromiumtricarbonyl fragment (Table 4). The nonplanarity of the selenophene ligand and the interaction with the chromium atom both contribute to this effect. In the calculated structure of the singlet insertion product, the six-membered chromaselena ring is not planar (Figure 10a) and the charge on the selenium, although less than in the (η^5-C_4H_4Se)$Cr(CO)_3$ compound, is significantly larger than in the uncoordinated ligand. In the calculated structure of the triplet species the chromaselena ring is essentially planar, and the efficient overlap of many orbitals, ligand and metal based, stabilizes the charge on the selenium (Figure 10b). Indeed the Mulliken charges on the selenophene-derived atoms (Se, C2, and C3) are similar to those of the uncoordinated ligand (Table 4). The charge on the chromium atom, however, is close to that in the 16-electron (η^5-C_4H_4Se)$Cr(CO)_2$ species.

The CO-loss species, (η^5-C_4H_4Se)$Cr(CO)_2$(S), is observed at room temperature in the TRIR experiments following excitation with 400 nm photons. Under similar irradiation no CO loss is observed in the matrix experiments. However, a similar observation to this was made in our studies on (η^6-C_6H_6)$Cr(CO)_3$, where the CO-loss species is observed in room-temperature solution following photolysis with 400 nm but not following 405 nm excitation in low-temperature matrixes.[21] This is explained by proposing the presence of a small thermal barrier to CO loss in the excited state, which at the low temperatures prevents CO loss. Higher energy photolysis (λ_{exc} = 365 nm) of (η^5-C_4H_4Se)$Cr(CO)_3$ in a dinitrogen matrix produced the

(20) (a) Schrock, R. R.; Shih, K. Y.; Dobbs, D. A.; Davis, W. M. *J. Am. Chem. Soc.* **1995**, *117*, 6609. (b) Detrich, J. L.; Reinaud, O. M.; Rheingold, A. L.; Theopold, K. H. *J. Am. Chem. Soc.* **1995**, *117*, 11745. (c) Carreón-Macedo, J. L.; Harvey, J. N. *J. Am. Chem. Soc.* **2004**, *126*, 5789. (d) Reiher, M. *Inorg. Chem.* **2002**, *41*, 6928–6935. (e) Reiher, M.; Salomon, O.; Hess, B A. *Theor. Chem. Acc.* **2001**, *107*, 48–55.

(21) Alamiry, M. A. H.; Boyle, N. M.; George, M. W.; Long, C.; Ronayne, K. L.; Towrie, M.; Pryce, M. T. Manuscript in preparation.

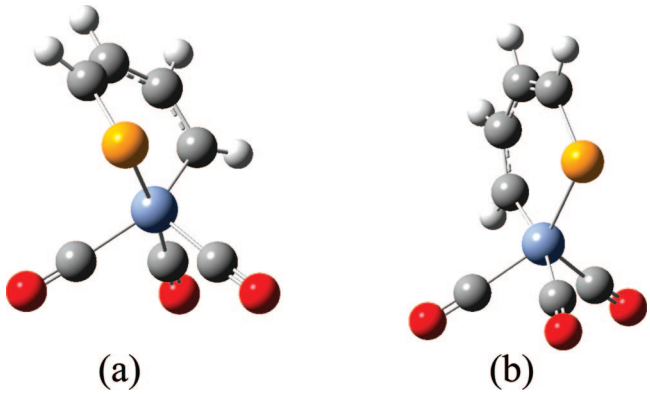

Figure 10. Calculated structures of (a) the singlet insertion product, $^1(C,Se\text{-}C_4H_4Se)Cr(CO)_3$, showing the chromium atom out of the plane of the C_4H_4Se unit and (b) the $^3(C,Se\text{-}C_4H_4Se)Cr(CO)_3$ species with a chromaselenabenzene type structure (both structures were optimized at the B3LYP/LANL2DZ+p model chemistry).

expected CO-loss species (η^5-C_4H_4Se)$Cr(CO)_2$, which interacts with the matrix environment to yield (η^5-C_4H_4Se)$Cr(CO)_2(N_2)$. Thus it is clear that (η^5-C_4H_4Se)$Cr(CO)_2$ has a singlet multiplicity. This suggests the existence of two energetically close excited states, the lower of which forms the insertion product, while the higher energy excited state produces the CO-loss species. Unfortunately the broadness of the initially produced bands in the ps TRIR experiments obscures the early time behavior of the system. No conclusions on whether the triplet species are formed from the intersystem crossing of an initially produced singlet excited state or simply by the relaxation of an initially produced singlet insertion species to a lower energy triplet species can be drawn from these results.

The efficiency of each of these processes can be estimated by examination of the intensities of the parent depletion in the TRIR experiments. Approximately 90% of the initial parent band depletion is recovered within the first 1 ns following excitation (Figure 7). This recovery is by way of an efficient nonradiative relaxation from the vibrationally hot excited state. The further recovery of parent absorptions by reaction of the CO-loss species with CO can be used to estimate the relative yields of the CO-loss species and the insertion product (Figure 9). Approximately 30% of the remaining parent bleach is restored by the reaction of (η^5-C_4H_4Se)$Cr(CO)_2$(S) with CO (S = *n*-heptane). Thus the overall quantum yield for CO loss is approximately 3%, and the total quantum yield for the insertion products is on the order of 7%.

Conclusion

A combination of matrix isolation, fast TRIR, and quantum chemical calculations has shown that low-energy excitation of (η^5-C_4H_4Se)$Cr(CO)_3$ can induce an opening of the selenophene ring and insertion of the chromium tricarbonyl fragment into the Se−C bond (Scheme 1). This process is complete within 1 ns of excitation. The unreactive nature of the resulting chromaselenabenzene (C,Se-C_4H_4Se)$Cr(CO)_3$ species is explained by its triplet character. This is the first example of a photoinduced insertion of a chromium tricarbonyl into a carbon−heteroatom bond and provides valuable insight into the activation mechanism for selenophene. It also provides further evidence for the importance of "spin blocking" in organometallic reaction mechanisms. Further work is ongoing on the analogous thiophene system to gauge the relevance of these results to the HDS process.

Scheme 1[a]

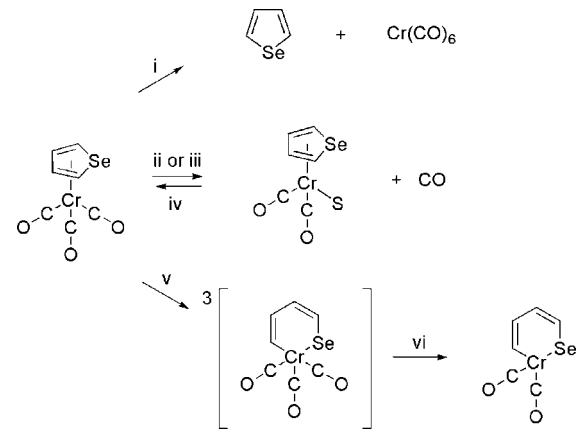

[a] Conditions: (i) $\lambda_{exc} > 340$ nm/CO-saturated (1 atm) C_6H_{12} or C_6D_{12} room temperature; (ii) $\lambda_{exc} = 400$ nm/S═CO-saturated (1 atm) C_7H_{16} room temperature; (iii) $\lambda_{exc} > 365$ nm/S═N_2 20 K; (iv) $k_2 = 5.8 \times 10^6$ dm^3 mol^{-1} s^{-1} at 298 K in CO-saturated (1 atm) C_7H_{16}; (v) $\lambda_{exc} = 400$ nm/S═CO-saturated (1 atm) C_7H_{16} room temperature; (vi) $\lambda_{exc} = 405$ nm/Ar matrix at 20 K; (vii) $\lambda_{exc} = 400$ nm/S═CO-saturated (1 atm) C_7H_{16} room temperature; (viii) $\lambda_{exc} = 365$ nm/Ar matrix at 20 K; (ix) $\lambda_{exc} > 500$ nm/Ar matrix at 20 K.

Experimental Section

Quantum Chemical Calculations. All calculations were carried out using the Gaussian 03 program revision C.02[22] running on a dual Xeon processor workstation (3.6 GHz) under Windows XP. The model chemistry employed in all calculations used the Becke three-parameter hybrid functionals,[23] using the correlation function of Lee, Yang, and Parr, which includes both local and nonlocal terms.[24] The LANL2DZ+p basis set was used for all metal complex calculations, which employs the Dunning/Huzinaga valence double-ζ functions for the first-row elements,[25] and the Los Alamos effective core potentials plus double-ζ functions on elements from Na to Bi.[26] An additional polarization function (+p) was added to the chromium and selenium atoms. The calculation on the selenophene ligand used the 6-31G** basis set to maintain consistency with the published electronic structure for this ligand.[13] Time-dependent DFT calculations used the geometry obtained from an optimization at the B3LYP/LANL2DZ+p model chemistry. The TDDFT calculations examined only the 10 lowest energy singlet states.

(22) Frisch, M. J.; Trucks, G. W.; Schlegel, H. B.; Scuseria, G. E.; Robb, M. A.; Cheeseman, J. R.; Montgomery, J. A., Jr.; Vreven, T.; Kudin,K. N.; Burant, J. C.; Millam, J. M.; Iyengar, S. S.; Tomasi, J.; Barone, V.; Mennucci, B.; Cossi, M.; Scalmani, G.; Rega, N.; Petersson, G. A.; Nakatsuji, H.; Hada, M.; Ehara, M.; Toyota, K.; Fukuda, R.; Hasegawa, J.; Ishida, M; Nakajima, T.; Honda, Y.; Kitao, O; Nakai, H.; Klene, M.; Li, X.; Knox, J. E.; Hratchian, H. P.; Cross, J. B.; Adamo, C.; Jaramillo, J.; Gomperts, R.; Stratmann, R. E.; Yazyev, O.; Austin, A. J.; Cammi, R; Pomelli, C.;J. Ochterski,W.; Ayala, P. Y.; Morokuma, K.; Voth, G. A.; Salvador, P.; Dannenberg, J. J.; Zakrzewski, V. G.; Dapprich, S.; Daniels, A. D.; Strain, M. C.; Farkas, O.; Malick, D. K.; Rabuck, A. D.; Raghavachari, K.; Foresman, J. B.; Ortiz, J. V.; Cui, Q.; Baboul, A. G.; Clifford, S.; Cioslowski, J.; Stefanov, B. B.; Liu, G.; Liashenko, A.; Piskorz, P.; Komaromi, I.; Martin, R. L.; Fox, D. J.; Keith, T.; Al-Laham, M. A.; Peng, C. Y.; Nanayakkara, A.; Challacombe, M.; Gill, P. M. W.; Johnson, B.; Chen, W.; Wong, M. W.; Gonzalez, C.; Pople, J. A. *Gaussian 03, Revision C.02*; Gaussian, Inc.: Wallingford, CT, 2004.

(23) Becke, A. D. *J. Chem. Phys.* **1993**, *98*, 5648.

(24) Lee, C.; Yang, W.; Parr, R. G. *Phys. Rev. B* **1988**, *37*, 785.

(25) Dunning, T. H., Jr.; Hay, R. J. *Modern Theoretical Chemistry*; Schaefer, H. F., III, Ed.; Plenum: New York, 1976; Vol. 3, pp 1−28.

(26) (a) Hay, P. J.; Wadt, W. R. *J. Chem. Phys.* **1985**, *82*, 270–283. (b) Wadt, W. R.; Hay, P. J. *J. Chem. Phys.* **1985**, *82*, 284. (c) Hay, R. J.; Wadt, W. R. *J. Chem. Phys.* **1985**, *82*, 299.

The GaussSum package[27] was used to obtain the contribution to specific Kohn−Sham orbitals made by specific molecule fragments, namely, the three CO ligands, the chromium and selenophene atoms, and the remaining CH fragments of the selenophene ligand (see Supporting Information for details).

Preparation of (η^5-C_4H_4Se)$Cr(CO)_3$. (η^5-C_4H_4Se)$Cr(CO)_3$ was prepared by thermal arene exchange of anthracene by selenophene from (η^6-$C_{14}H_{10}$)$Cr(CO)_3$ using a modification of the published method.[28] A solution of (η^6-$C_{14}H_{10}$)$Cr(CO)_3$ (400 mg, 1.3 mmol) and C_4H_4Se (3 g, 23 mmol) in 2.5 mL of freshly distilled tetrahydrofuran (THF) was heated to reflux temperature under an argon atmosphere for 75 min. The solvent was then removed under reduced pressure at room temperature, yielding an orange solid. The crude material was chromatographed on neutral silica eluting with 3:1 petroleum ether/dichloromethane. Following elution of the first band of unreacted (η^6-$C_{14}H_{10}$)$Cr(CO)_3$ the mobile phase was changed to pure dichloromethane. The product eluted as the second band. Removal of the solvent under reduced pressure yielded a dark red powder. The crude product was recrystallized from toluene/*n*-pentane, yielding 197 mg of product, representing a 57% yield based on (η^6-$C_{14}H_{10}$)$Cr(CO)_3$. Spectroscopic data were in accordance with those previously reported.[28]

Preparation of (η^6-$C_{14}H_{10}$)$Cr(CO)_3$. A solution of $Cr(CO)_6$ (400 mg, 1.8 mmol) and $C_{14}H_{10}$ (3.4 g, 19 mmol) in dibutyl ether (12 mL) containing THF (1 mL) was heated to its reflux temperature for 6 h with continual stirring. The resulting dark red solution was then cooled and filtered through Celite. The solvent was then removed under reduced pressure. The resulting crude product was chromatographed on silica using 2:1 petroleum ether/dichloromethane mobile, (η^6-$C_{14}H_{10}$)$Cr(CO)_3$ eluting as a red band. The product was then recrystallized from toluene/*n*-pentane yielding 141 mg (0.44 mmol), representing a 41% yield based on $Cr(CO)_6$. Spectroscopic data were in accordance with those previously reported.[29]

Sample Preparation. All manipulations were carried out under an argon atmosphere. Spectroscopic grade solvents (*n*-pentane and cyclohexane) were used as obtained (Aldrich spectroscopic grade). Gases used for the matrix experiments (Ar, N_2, and CO) were BOC research grade (99.999% purity). Infrared spectra were recorded on a Perkin-Elmer 2000 FT-IR spectrometer using sodium chloride windows ($d = 0.1$ mm) and spectroscopic grade cyclohexane, *n*-pentane, or dichloromethane. NMR (^1H and ^{13}C) spectra were measured on a Brüker model AC400 MHz spectrometer in appropriate deuterated solvents at room temperature. The peaks were calibrated according to the external TMS standard. UV/vis spectra were recorded on a Hewlett-Packard 8452A photodiode array spectrometer, using quartz cells of 1 cm path length.

Matrix Isolation Apparatus. The matrix setup was described previously.[30] Briefly, the matrix isolation apparatus consists of a closed cycle helium refrigerator, sample window, shroud, deposition tube, gas mixing chamber, gas inlet, backing pump, diffusion pump, and temperature control unit. Matrixes were deposited onto a CaF_2 window cooled to 20 K, with matching outer windows on the vacuum shroud. Samples for infrared spectroscopy were deposited onto a CaF_2 window cooled by an X CS202 closed-cycle refrigerator to 20 K. A thermocouple embedded into a cavity beside the window and connected to the temperature control unit maintains the temperature. The window is cooled by a closed cycle helium refrigerator (Air Products), mounted via a double O-ring seal in a stainless steel vacuum shroud. The system pumps to 8×10^{-4} mbar prior to cooling and achieves 10^{-7} mbar upon cooling to 20 K. Host gases (Cryo Service) are deposited onto a window via a needle valve. For mixed gas matrixes, the gases are mixed in the correct ratio in the stainless steel mixing chamber prior to deposition. A ratio of sample molecule to host matrix in the region 1:2000 is desirable. Typically the rate of gas deposition of 0.6 Torr per minute achieves sufficient dilution of analyte in the matrix. All manipulations were carried out under an argon atmosphere. (η^5-C_4H_4Se)$Cr(CO)_3$ was sublimed from a right-angled tube at 334 K as the gas stream entered the vacuum shroud. The sample was deposited onto the windows at 20 K and monitored in the infrared until the absorbance reading of one of the metal−carbonyl bands was approximately 1 AU. When the required absorbance was achieved, the samples were photolyzed and IR changes monitored on a Perkin-Elmer Spectrum One FTIR spectrophotometer (typically 16 scans at 1 cm^{-1} resolution). Photolysis wavelengths were selected with interference or cutoff filters (λ_{exc} = 405, 365, using a 250 W Xe/Hg lamp, > 410 or >500 nm) used in conjunction with a 250 W Xe lamp, both supplied by Oriel Scientific.

Picosecond TRIR Apparatus. The TRIR apparatus is located at Nottingham University and is based upon the PIRATE facility at the Rutherford Appleton Laboratory.[31] A commercial Ti:sapphire oscillator (MaiTai)/regenerative amplifier system (Spitfire Pro, Spectra Physics) is used to generate 800 nm laser pulses with an energy of 2.3 mJ at a repetition rate of 1 kHz. This output is divided into two parts with approximately the same energy pumping either a TP-1 harmonic generator (TimePlate Tripler, Minioptic Technology, Inc.) to generate UV pulses (400 or 267 nm) or a TOPAS-C OPA (Light Conversion) with a DFG (difference frequency generator) unit to produce a tunable mid-IR pulse with a spectral bandwidth of 180 cm^{-1} and a pulse energy of ca. 2 μJ at 2000 cm^{-1}. The IR pulse passes through a Ge beam splitter. Half of the IR pulse is reflected onto a single-element MCT detector (Kolmar Technology) to serve as a reference, and the other half serves as the probe beam, which is focused and overlaps with the pump beam at the sample position. The UV−vis pump pulse is optically delayed (up to 3 ns) by a translation stage (LMA Actuator, Aerotech) and focused onto the sample with a quartz lens. The polarization of the pump pulse is set at the magic angle (54.7°) relative to the probe pulse to recover the isotropic absorption spectrum. For a measurement with a longer time delay, a Q-switched Nd:YVO laser (ACE-25QSPXHP/MOPA, Advanced Optical Technology, UK) is employed as a pump source, which is synchronized to the Spitfire Pro amplifier. The delay between pump and probe pulses can be controlled with a pulse generator (DG535, Stanford Research System) from 0.5 ns to 100 μs. The broadband transmitted probe pulse is detected with a HgCdTe array detector (Infrared Associates), which consists of 128 elements (1 mm high, 0.25 mm wide). The array detector is mounted in the focal plane of a 250 mm IR spectrograph (DK240, Spectra Product) with a 150 g/mm grating, resulting in a spectral resolution of ca. 4 cm^{-1}, and a 300 g/mm grating, giving a spectral resolution of ca. 2 cm^{-1} at 2000 cm^{-1}. The signals from the array detector elements and the single-element detector were amplified with

(27) O'Boyle, N. M. *GaussSum 2.0*, 2006. Available at http://gausssum.sf.net.

(28) Loft, M. S.; Mowlem, T. J.; Widdowson, D. A. *J. Chem. Soc., Perkin Trans.* **1995**, 97.

(29) Morley, J. A.; Woolsey, N. F. *J. Org. Chem.* **1992**, *57*, 6487.

(30) Long, C; Maher, K.; Pryce, M. T. *J. Organomet. Chem.* **2006**, *691*, 3298.

(31) Towrie, M.; Grills, D. C.; Dyer, J.; Weinstein, J. A.; Matousek, P.; Barton, R.; Bailey, P. D.; Subramaniam, N.; Kwok, W. M.; Ma, C. S.; Phillips, D.; Parker, A. W.; George, M. W. *Appl. Spectrosc.* **2003**, *57*, 367.

a 144-channel amplifier and digitized by a 16-bit analogue-to-digital converter (IR-0144, Infrared Systems Development Corp.). The pump-induced change in the absorbance ΔA is determined by chopping the pump pulse at half the repetition frequency of the laser and calculating the ratio between the pump-on and pump-off transmittance. Chopping the excitation light pulse greatly reduces long-term instrumental drift. The signal from the single element detector serves as reference to normalize the shot-to-shot fluctuation. The pump beam size ($\sim$500 μm diameter) is larger than the probe spot ($\sim$200 μm diameter) to ensure spatially uniform photoexcitation over the area of the probe pulse. A Harrick flowing solution cell with 2 mm thick CaF_2 windows (path length: 0.5 mm) is mounted on a motorized cell mount, which moves the cell rapidly in *x* and *y* dimensions throughout the experiment. Consequently each laser pulse illuminates a different volume of the sample, reducing overheating and degradation of the sample solution.

Acknowledgment. The authors gratefully acknowledge the support of Enterprise Ireland (P.B. and J.McK.) and Dublin Co. Council (P.B). Dr. A. Denise Rooney is thanked for helpful discussions.

Supporting Information Available: Tables listing atomic coordinates, internuclear distances, normal modes of (η^5-C_4H_4Se)$Cr(CO)_3$ (singlet and triplet), (η^5-C_4H_4Se)$Cr(CO)_2$ (singlet and triplet), (*C,Se*-C_4H_4Se)$Cr(CO)_3$ (singlet and triplet), (*C,Se*-C_4H_4Se)$Cr(CO)_2$ (singlet and triplet), (η^1-*C2*-C_4H_4Se)$Cr(CO)_3$ (triplet), and C_4H_4Se (singlet, B3LYP/6311G**), and contributions of Cr, Se, CO_3, and C_4H_4 to Kohn−Sham orbitals in (η^5-C_4H_4Se)$Cr(CO)_3$. Spectroscopic changes observed in steady-state photolysis experiments in the presence of CO and pyridine (UV and IR) are also presented. This material is available free of charge via the Internet at http://pubs.acs.org.

OM7011979